Solid State Communications 204 (2015) 1–4

Contents lists available at ScienceDirect

Solid State Communications

journal homepage: www.elsevier.com/locate/ssc

Structure, magnetic and electrical properties of disordered double perovskite Pb_2CrMoO_6

H.F. Zhao [a], L.P. Cao [a], Y.J. Song [a,b], S.M. Feng [a], X. Shen [a], X.D. Ni [b], Y. Yao [a], Y.G. Wang [a], C.Q. Jin [a], R.C. Yu [a,*]

[a] Beijing National Laboratory for Condensed Matter Physics, Institute of Physics, Chinese Academy of Sciences, Beijing 100190, China
[b] Department of Physics, University of Science and Technology Beijing, Beijing 100083, China

ARTICLE INFO

Article history:
Received 2 September 2014
Received in revised form
6 November 2014
Accepted 2 December 2014
Communicated by T.T.M. Palstra
Available online 10 December 2014

Keywords:
A. Double perovskite
B. High pressure
D. Weak ferromagnetism

ABSTRACT

We prepared Pb_2CrMoO_6 under high pressure and high temperature. The sample has a heavily or fully disordered double perovskite structure (*Pm-3m*, $a=3.9472$ Å). It shows a weak ferromagnetic behavior ($T_C\sim33$ K) and a significant low magnetization ($\sim0.095\ \mu_B$/f.u. at 7 T and 5 K), which is discussed based on the cation disorder. The temperature dependence of the electrical resistivity of Pb_2CrMoO_6 exhibits a semiconducting behavior, which could be well understood by the 3D variable range hopping model. No significant magnetoresistance was observed in this sample.

1. Introduction

Double perovskite oxides $A_2BB'O_6$ have attracted considerable attention since the discovery of colossal magnetoresistance in Sr_2FeMoO_6 [1–3]. As a most studied member of $A_2BB'O_6$ family, Sr_2FeMoO_6 is a half-metallic ferrimagnet with a high Curie temperature (T_C) of ~415 K, and low field magnetoresistance of Sr_2FeMoO_6 is attributed to the spin-polarized electron scattering at grain or magnetic domain boundaries. The large room-temperature magnetoresistance makes such materials a good candidate for the applications including nonvolatile magnetic random access memory, magnetic read heads for hard drives and magnetic sensor, etc.

Nowadays, experimental and theoretical studies are still being carried out to seek $A_2BB'O_6$ materials with optimized properties. Up to now, the $A_2BB'O_6$ (A=Ca, Sr, Ba; B=Cr, Fe; B′=Mo, W, Re) analogues of Sr_2FeMoO_6 have been systematically investigated [4–6], while the Pb-based analogues are less studied due to the toxicity of lead, although the ionic radius of Pb^{2+} is very close to that of Sr^{2+}. Meanwhile, unlike the alkaline earth elements, Pb ion has additional 6 s lone pair electrons, which is usually related to the ferroelectricity of perovskite materials [7]. Recently, first-principle calculations performed by Gong et al. [8] predict that the ordered double perovskite Pb_2CrMoO_6 is a half-metallic ferrimagnet with a $T_C\geq480$ K. However, no experimental study of Pb_2CrMoO_6 has been reported up to now. So, we attempted to synthesize Pb_2CrMoO_6, and finally got a single phase with the nominal formula, then investigated its structural, magnetic and transport properties.

2. Experimental

Our attempts to synthesize Pb_2CrMoO_6 at ambient pressure (sintering of stoichiometric mixture of raw materials in vacuum, sintering in a flowing Ar/H_2 gas) were unsuccessful. However, single-phase Pb_2CrMoO_6 could be fabricated via a high pressure-high temperature synthesis route. Stoichiometric mixture of PbO, Cr_2O_3, Mo and MoO_3 was ground within an agate mortar for 1 h, pressed into pellets of Φ6 mm, and then enveloped in Au foil. The ultimate synthesis was conducted in a cubic anvil-type apparatus at about 880 °C and 5.5 GPa for 30 min. Pressure was released slowly after quenching the specimen to room temperature. The cation stoichiometry of the synthesized sample was examined with inductively coupled plasma-atomic emission spectrometry (ICP-AES) (IRIS Advantage, Thermo Elemental).

The crystal structure of the ceramics were characterized by powder X-ray diffraction (XRD) (X'Pert Pro, Philips) with Cu *Kα* radiation and transmission electron microscopy (TEM) (Tecnai F20 FEG, Gatan) analysis. For the Pb_2CrMoO_6 slice is fragile, the sample

* Corresponding author at: Beijing National Laboratory for Condensed Matter Physics, Room 1025, Building M, Zhongguancun South 3rd Street, Beijing 100190, China. Tel.: +86 10 82649159.
E-mail address: rcyu@aphy.iphy.ac.cn (R.C. Yu).

http://dx.doi.org/10.1016/j.ssc.2014.12.001
0038-1098/

for TEM observation was prepared as a cross-sectional TEM sample with single crystal Si as the supporting material.

The magnetic property measurements were performed on Quantum Design Physical Property Measurement System (PPMS). In the electrical property measurements, temperature control and measurement were performed on an Oxford Maglab measuring system, the resistivity data were measured with an external Keithley 2182A nanovoltmeter.

3. Results and discussion

The normalized atomic ratio of Pb:Cr:Mo is about 51.80:23.63:24.57 measured by ICP-AES and agrees well with the nominal value of 50:25:25. The XRD pattern of the synthesized Pb_2CrMoO_6 can be indexed with a simple cubic unit cell with the parameter $a=3.9472$ Å using WinPLOTR and DICVOL [9] as shown in Fig. 1. Since no systematic absence is observed on the XRD pattern, there are only 5 possible space groups and there is one-to-one correspondence between these space groups and the 5 point groups of cubic lattice. For a certain point group, the exhibited symmetries at different zone axes, i.e. the diffraction group (DG), are different. For different diffraction groups, the exhibited symmetries in the convergent beam patterns (such as whole pattern, dark field, bright field and $\pm$G) are different. Buxton et al. [10] established the relationships among point groups, diffraction groups along different directions and the exhibited symmetry in CBED patterns. Thus, by observing the symmetry in CBED patterns along different orientations of the sample, the diffraction group could be determined and then the point group is concluded. At last, the space group can be uniquely determined with regard to the one-to-one correspondence mentioned before. The correspondence among the 5 space groups, point groups, diffraction groups along [1 1 1] and [0 0 1] orientations, and whole pattern symmetry (WPS) is summarized in Fig. 2(a). For there are mirror planes on the whole pattern of the [1 1 1] orientation, the possible space groups are reduced to *P-43m* and *Pm-3m*. Since the whole pattern of the [0 0 1] orientation exhibits 4-fold symmetry rather than 2-fold symmetry, the space group *P-43m* is also excluded. As a result, the space group of the sample is uniquely determined to be *Pm-3m* (221). To make sure our result is representative, we acquired the CBED patterns from many particles and all of them give the same information.

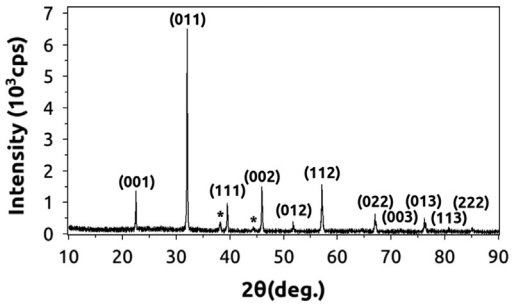

Fig. 1. XRD pattern of Pb_2CrMoO_6. The peaks marked with * are from Au.

In the case of Sr_2FeMoO_6 [11], although the order-related peaks are totally absent, Rietveld analysis of the XRD pattern indicates the presence of a significant extent of ordering at the Fe/Mo site. However, we didn't find the evidence of the presence of the Cr/Mo ordering in our samples during our TEM work. In a word, our samples crystallize in a heavily or completely disordered double perovskite phase, different from A_2BMoO_6 (A=Ca, Sr, Ba; B=Cr, Fe); [5,12,13], but same as Ca_2CrMoO_6 [14], Pb_2FeMoO_6 [15].

Fig. 3 displays the temperature dependence of zero-field-cooled (ZFC) and field-cooled (FC) magnetization of Pb_2CrMoO_6 under 1000 Oe. The magnetization behavior of Pb_2CrMoO_6 is almost the same as that of Ba_2CrMoO_6 [13]. With decreasing temperature, the ZFC and FC curves start splitting below $\sim$30 K, and the ZFC curve shows a narrow cusp at $\sim$24 K, while the FC curve increases monotonically. The inverse magnetization is not Curie–Weiss like up to 300 K, and the curvature is consistent with short range ferromagnetic interactions. And the lack of magnetic saturation below the transition temperature also reveals that the ferromagnetism cannot be long-range order. The transition temperature ($T_C\sim$33 K) is obtained from the inflection point of the first

a

Space group		*P*23 (195)	*Pm*$\bar{3}$ (200)	*P*432 (207)	*P*$\bar{4}$3*m* (215)	*Pm*$\bar{3}$*m* (221)
Point group		23	*m*$\bar{3}$	432	$\bar{4}$3*m*	*m*$\bar{3}$*m*
<111>	DG	3	6_R	$3m_R$	3*m*	6_Rmm_R
	WPS	3	3	3	3*m*	3*m*
<001>	DG	$2m_Rm_R$	$2mm1_R$	$4m_Rm_R$	4_Rmm_R	$4mm1_R$
	WPS	2	2*mm*	4	2*mm*	4*mm*

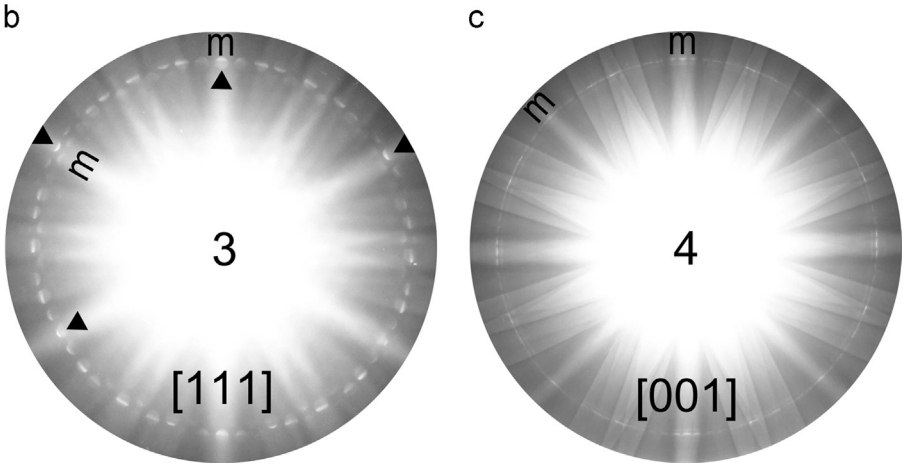

Fig. 2. (a) The correspondence among the 5 space groups with no systematic absence, point groups, diffraction groups (DG) along [1 1 1] and [0 0 1] orientations, and whole pattern symmetry (WPS). The experimental whole CBED patterns along (b) [1 1 1] and (c) [0 0 1] orientations were obtained at 200 kV and 160 kV, respectively.

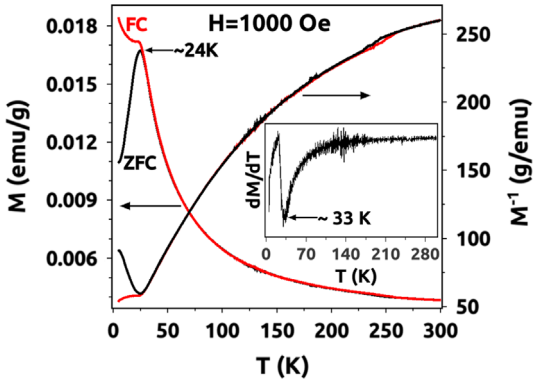

Fig. 3. ZFC and FC magnetization as a function of temperature under 1000 Oe. The inset shows dM/dT vs. temperature plot for FC magnetization.

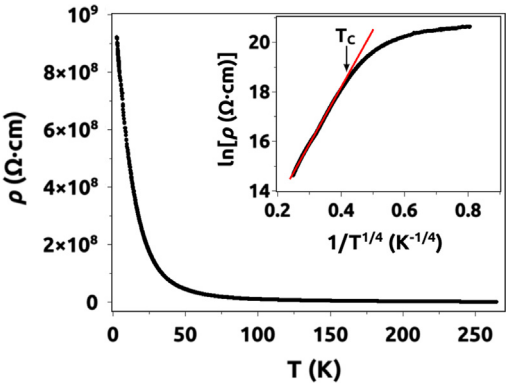

Fig. 5. Temperature dependence of the resistivity of Pb_2CrMoO_6 from 2 K to 265 K at zero magnetic field. The inset shows the $\ln\rho - 1/T^{1/4}$ fitting results by VRH model.

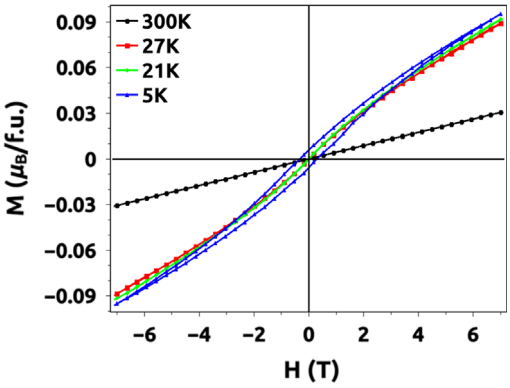

Fig. 4. M–H curves of Pb_2CrMoO_6 at 5 K, 21 K, 27 K and 300 K, respectively.

derivative of FC magnetization, which is related to the average intensity of magnetic interactions [15,16].

The isothermal magnetization curves (M–H) of Pb_2CrMoO_6 at different temperatures are shown in Fig. 4 with magnetic field up to 7 T. The M–H curve exhibits a clear hysteresis loop at 5 K with a very small remanent magnetization of ~0.006 μ_B/f.u., indicating the presence of a weak ferromagnetism phenomenon in Pb_2CrMoO_6. The highest value of magnetic moment at 7 T is only ~0.095 μ_B/f.u., which is considerably lower than the spin-only value (2 μ_B/f.u.) of ferrimagnetically coupled Cr^{3+} and Mo^{5+} ions [17]. Another interesting feature at low temperature is the unsaturated behavior of the M–H curve even at higher fields. These phenomena should result from the complex physics caused by the Cr/Mo disorder.

The slope of M is found to decrease with increasing $|H|$ at 21 K and 27 K without a hysteresis loop. This indicates the spin moments are gradually aligned with increasing H. As a result, the scattering of charge carriers by spin moments is expected to decrease with increasing H [18]. However, maybe due to the weak magnetization [19], no significant magnetoresistance was observed in our sample down to 2 K under 4 T. At a temperature higher than T_c ($T > 33$ K), the M–H behavior is linear, corresponding to a paramagnetic state.

The electrical behavior of Pb_2CrMoO_6 is semiconducting, as shown in Fig. 5. In order to understand the transport mechanism in this compound, a thermally activated model, $\rho(T) = \rho_0 \exp(E_0/kT)$ and a 3-dimensional variable range hopping model (VRH) [20] $\rho(T) = \rho_0 \exp(T_0/T)^{1/4}$ are used to fit the resistivity data above T_c (from 40 to 265 K). The VRH model gives a better fit than the other. The inset of Fig. 5 shows the fitting results of $\ln\rho - 1/T^{1/4}$ according to this model. The fitted parameters of ρ_0 (pre-exponential factor) and T_0 (characteristic Mott temperature) are 8020 Ω cm and 2.80×10^5 K, respectively. In the VRH model, the parameter T_0 is related to the inverse localization length α, by the expression, $kT_0 = 18\alpha^3/3N(E_F)$, where $N(E_F)$ is the density of states at the Fermi energy. So, a large T_0 corresponds to a small localization length, suggesting the electrons are highly localized within the sample [20]. Besides, T_0 can also be considered as the extent of disorder in the disordered region [21]. A large value of T_0 indicates that Cr^{3+} and Mo^{5+} arrange in some degree of disordering, which agrees with the previous structural and magnetic analysis results.

In summary, double perovskite Pb_2CrMoO_6 was synthesized by a high pressure and high temperature method. The sample crystallizes in a simple cubic structure ($a = 3.9472$ Å), indicating Cr^{3+} and Mo^{5+} are heavily or fully disordered in the B-site. The magnetic properties correspond to a weak ferromagnet with $T_c \sim 33$ K. The significant low magnetization (~ 0.095 μ_B/f.u. at 7 T and 5 K) was discussed based on the cation disorder. The transport property measurement of Pb_2CrMoO_6 shows a semiconducting behavior, which could be well described by the VRH model. No significant magnetoresistance was observed down to 2 K at 4 T.

Acknowledgements

This work was supported by the State Key Development Program for Basic Research of China (Grant no. 2012CB932302) and the National Natural Science Foundation of China (Grant no. 11174336).

References

[1] K. Kobayashi, T. Kimura, H. Sawada, Nature 395 (1998) 677.
[2] D. Serrate, J.M. De Teresa, M.R. Ibarra, J. Phys. Condens. Matter. 19 (2007) 023201.
[3] D. Sarma, Curr. Opin. Solid State Mater. Sci. 5 (2001) 261.
[4] M. Retuerto, F. Jiménez-Villacorta, M.J. Martínez-Lope, Y. Huttel, E. Roman, M.T. Fernández-Díaz, J.a. Alonso, Phys. Chem. Chem. Phys. 12 (2010) 13616.
[5] R.P. Borges, R.M. Thomas, C. Cullinan, J.M.D. Coey, R. Suryanarayanan, L. Ben-Dor, L. Pinsard-Gaudart, A. Revcolevschi, J. Phys. Condens. Matter 11 (1999) L445.
[6] T.S. Chan, J.-F. Lee, R.S. Liu, J. Phys. Conf. Ser. 190 (2009) 012095.
[7] R. Seshadri, N.A. Hill, Chem. Mater. 13 (2001) 2892.
[8] S. Gong, P. Chen, B.G. Liu, J. Magn. Magn. Mater. 349 (2014) 74.
[9] A. Boultif, D. Louër, J. Appl. Cryst. 37 (2004) 724.
[10] B.F. Buxton, J.a. Eades, J.W. Steeds, G.M. Rackham, Philos. Trans. R. Soc. London, Ser. A 281 (1976) 171.
[11] D.D. Sarma, E.V. Sampathkumaran, S. Ray, R. Nagarajan, S. Majumdar, A. Kumar, G. Nalini, T.N. Guru Row, Solid State Commun. 114 (2000) 465.
[12] A. Arulraj, K. Ramesha, J. Gopalakrishnan, C.N.R. Rao, J. Solid State Chem. 155 (2000) 233.
[13] F. Sher, J.P. Attfield, Solid State Sci. 8 (2006) 277.
[14] M.J. Martínez-Lope, J.a. Alonso, M.T. Casais, M. García-Hernández, V. Pomjakushin, J. Solid State Chem. 179 (2006) 2506.
[15] X. Yuan, M. Xu, Y. Chen, Appl. Phys. Lett. 103 (2013) 052411.

[16] J. Navarro, J. Nogués, J. Muñoz, J. Fontcuberta, Phys. Rev. B: Condens. Matter 67 (2003) 174416.

[17] M. Musa Saad H.-E., M. El-Hagary, J Magn. Magn. Mater. 360 (2014) 229.

[18] J. Sugiyama, C. Xia, T. Tani, Phys. Rev. B: Condens. Matter 67 (2003) 104410.

[19] M. García-Hernández, J. Martínez, M. Martínez-Lope, M. Casais, J. Alonso, Phys. Rev. Lett. 86 (2001) 2443.

[20] F. Sher, A. Venimadhav, M.G. Blamire, B. Dabrowski, S. Kolesnik, J.P. Attfield, Solid State Sci. 7 (2005) 912.

[21] Y. Zhai, J. Qiao, G. Huo, S. Han, J. Magn. Magn. Mater. 324 (2012) 2006.